Promega

Tackle Your Sample Preparation, Amplification and Analysis Challenges

Learn helpful tips, tricks & technique refreshers with our free eBook

Looking for a quick technique refresher or a way to support your mentee? Need to adapt an existing technology or need a unique formulation, but not sure where to start? Our Custom Solutions eBook can help.

This eBook was designed as an educational resource to address your sample preparation, amplification and analysis challenges in the lab. It also offers insight into the benefits and value of partnering with a Custom/OEM supplier.

To Download the Free eBook, Scan the QR Code or Visit:

www.promega.com/CustomSolutionsEbook

Let's TALK CUSTOM

DOI: 10.1002/mas.21797

REVIEW ARTICLE

WILEY

Mass spectrometry in organic and bio-organic catalysis: Using thermochemical properties to lend insight into mechanism

Damon J. Hinz | **Lanxin Zhang** | **Jeehiun K. Lee**

Department of Chemistry and Chemical Biology, Rutgers, The State University of New Jersey, New Brunswick, New Jersey, USA

Correspondence
Jeehiun K. Lee, Department of Chemistry and Chemical Biology, Rutgers, The State University of New Jersey, New Brunswick, NJ 08901, USA.
Email: jee.lee@rutgers.edu

Abstract

In this review, we discuss gas phase experimentation centered on the measurement of acidity and proton affinity of substrates that are useful for understanding catalytic mechanisms. The review is divided into two parts. The first covers examples of organocatalysis, while the second focuses on biological catalysis. The utility of gas phase acidity and basicity values for lending insight into mechanisms of catalysis is highlighted.

KEYWORDS

acidity, enzymes, organocatalysts, proton affinity, reaction mechanisms

1 | INTRODUCTION

Gas-phase techniques are important tools in the study of organic and bio-organic reactions, allowing for the study of reactivity in the absence of solvent. Because mass spectrometry (MS) is performed in the gas-phase, one can utilize MS to examine inherent reactivity, in the absence of solvent. Using MS to study organic ion/molecule reactions has a long history, beginning with seminal early studies by Beauchamp, Bowers, Brauman, and DePuy, among others (Comita & Brauman, 1985; DePuy, 2002; Feng & Gronert, 2000; Gronert, 2001). As the field has progressed, advancements in instrumentation have allowed for the study of more complicated systems, such as those involving organic and biological catalysis.

Studying any process in the gas-phase, using MS, requires ionic species for detection. One set of thermochemical values that can be accurately measured and quantified by MS is acidity and proton affinity (PA). Furthermore, it has been shown that trends in acidity and PA can lend significant insight into related reaction mechanisms and processes. In this review, we discuss gas-phase experimentation centered on the measurement of acidity and PA of substrates that are useful for organocatalytic and enzymatic chemistry.

2 | ORGANOCATALYSTS

While organometallic catalysis may appear to dominate the field of catalytic chemistry, organocatalysts have been going through a revolution in recent years (List, 2007). In comparison to transition metal catalysts, organic catalysts have several clear benefits: tendency to be less moisture sensitive, affordability, availability, and lower toxicity (Dondoni & Massi, 2008; MacMillan, 2008). Because organocatalysts are less commonly ionic or easily ionizable, they are more of a challenge to study via MS than transition metal-containing species. However, several studies in recent years show the power that the gas-phase can wield in revealing mechanistic insights.

2.1 | *N*-Heterocyclic carbenes (NHCs)

NHCs (Figure 1) are used extensively as ligands in organometallic reactions, and as standalone organocatalysts. As organocatalysts, they predominantly act as nucleophiles in *Umpolung* reactions involving carbonyl species. Perhaps most famously, NHCs catalyze the benzoin condensation and the related Stetter reaction (Figure 2) (Breslow, 1958; Stetter & Kuhlmann, 1974). In the case of the benzoin condensation, the NHC nucleophilically

catalyzes the coupling of two benzaldehyde species, to form an α-hydroxyketone. In the related Stetter reaction, NHCs nucleophilically catalyze the coupling of an aldehyde to an α,β-unsaturated carbonyl. Both reactions have significant synthetic implications, and stereoselective versions of each have been developed (Enders & Balensiefer, 2004; Hopkinson et al., 2014; Moore & Rovis, 2009).

Several studies in recent years have tackled the characterization of the thermochemical properties of NHCs in the gas-phase. The first measurement of an NHC PA was accomplished by Cooks and coworkers. Using the kinetic method, the Cooks group measured the PA of 1-ethyl-3-methylimidazol-2-ylidene (Figure 3) (H. Chen et al., 2005). In the Cooks kinetic method, a dimer is formed in solution between reference acids or bases and the molecule of interest. This dimer is then subjected to collision-induced dissociation (CID) at different energies, and the ratio of the signals of the protonated monomers is measured. The PA of the molecule of interest can be determined from the ratio (Figure 4). In this study, the PA of 1-ethyl-3-methylimidazol-2-ylidene was determined to be $251.3 \pm 4\,\text{kcal mol}^{-1}$. While this initial study did not focus on the NHC as a catalyst, it was the first gas-phase measurement of the PA of an NHC, and revealed the high gas-phase basicity of this NHC.

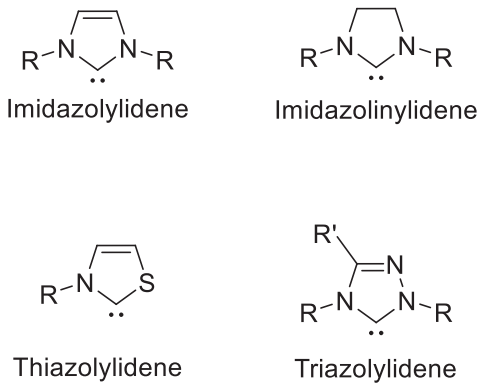

FIGURE 1 Common *N*-heterocyclic carbene scaffolds

Lee et al. expanded on the Cooks work by using a bracketing method to redetermine the PA of 1-ethyl-3-methylimidazol-2-ylidene, and to assess 1,3-dimethylimidazol-2-ylidene (Figure 3) (Liu et al., 2011a). Inconsistencies between the experimentally determined PA of 1-ethyl-3-methylimidazol-2-ylidene and the computed PA (using B3LYP/6-31+G(d) and MP2/6-311+G(2d,p)//B3LYP/6-31+G(d)) led to suspicions that the Cooks kinetic measurement might be a bit low. To test this hypothesis, a quadrupole ion trap was modified to allow for the introduction of neutral reference compounds, so that the NHC PA could be bracketed. In this method, PAs are determined by assessing the occurrence or absence of proton transfer with various reference bases (Figure 5). Using bracketing, the Lee group determined that 1-ethyl-3-methylimidazol-2-ylidene has a PA between 254.0 and $260.6\,\text{kcal mol}^{-1}$. 1,3-Dimethylimidazol-2-ylidene was found to have a PA between 257.4 and $260.6\,\text{kcal mol}^{-1}$. These values are consistent with the calculated PAs. In general, measurement of NHC PAs is challenging; the relatively high basicity means that there is a dearth of available reference compounds. Overall, these studies by the Cooks and Lee groups were the first to show that NHCs are strong bases in the gas-phase.

Rovis, Lee, and coworkers recently used the same modified quadrupole ion trap to study correlations between a series of triazolylidene NHC catalysts and the stereoselectivity of an intramolecular Stetter reaction (Niu et al., 2017). The proposed mechanism of the Stetter reaction is shown in Figure 6. In this mechanism, the

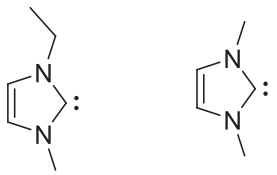

FIGURE 3 1-Ethyl-3-methylimidazol-2-ylidene (left) and 1,3-dimethylimidazol-2-ylidene (right)

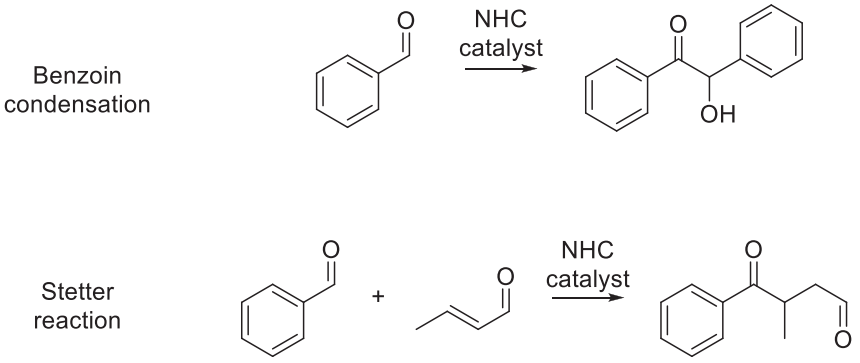

FIGURE 2 Benzoin condensation and Stetter reaction

$$\ln\left(\frac{k_1}{k_2}\right) = \ln\left(\frac{[\boldsymbol{B_i}\cdot H^+]}{[\boldsymbol{A}\cdot H^+]}\right) = \ln\left(\frac{[^x\boldsymbol{B}_i\cdot H^+]}{[^x\boldsymbol{A}\cdot H^+]}\right) \approx \frac{\Delta PA(\boldsymbol{A})}{RT_{eff}} = \frac{PA(\boldsymbol{B}_i)}{RT_{eff}} - \frac{PA(\boldsymbol{A})}{RT_{eff}}$$

FIGURE 4 Cooks kinetic method equation. $^x\mathbf{B}_i\bullet H^+$ is the intensity of the signal of the protonated base of interest, $^x\mathbf{A}\bullet H^+$ is the intensity of the signal of the protonated reference. R is the gas constant. T_{eff} is the average internal energy of the ion complexes that dissociate within the time window of the experiment.

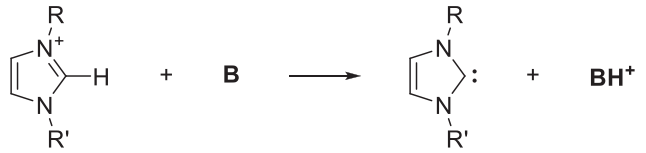

FIGURE 5 Bracketing of the acidity of a protonated imidazole. **B** is a reference base with known PA. The protonated imidazolylidene is allowed to react with a series of reference bases B whose PAs are known. The presence or absence of proton transfer is used to bracket the imidazolylidene PA. PA, proton affinity.

NHC catalyst nucleophilically attacks the carbonyl carbon of an aldehyde to form an alkoxide. A 1,2-proton transfer then occurs, yielding the "Breslow intermediate," which is relatively more thermodynamically stable than the alkoxide. This Breslow intermediate then adds nucleophilically to an α,β−unsaturated carbonyl. The Stetter reaction can yield 1,4-dicarbonyl compounds as shown in Figure 6, as well 4-ketocarboxylic acids, and the corresponding nitriles. Rovis and Lee first focused on a Stetter reaction between cinnamaldehyde and a series of nitroalkenes (Figure 7). In this reaction, a protonated triazolium precatalyst is added (Figure 7); when deprotonated, this precatalyst becomes the NHC catalyst. Rovis and Lee examined the gas-phase acidity of the precatalyst experimentally and computationally to probe the electronic effect of various aryl substituents on the gas-phase acidity, to ascertain whether any insights into catalyst ability could be gained.

Correlation was found between the gas-phase acidity of the NHC precatalyst and the *syn* to *anti* ratio of the products. This is an example of where gas-phase properties inform a solution-phase reaction. The authors note that the gas-phase acidities have a wider range than the solution-phase values, which make trends and correlations easier to ascertain. The more acidic the protonated NHC precatalyst, the more likely the *syn* product. Using DFT calculations, the authors also proposed and supported a hypothesis that the more acidic precatalysts favor the *Z* geometry of the Breslow intermediate, which ultimately leads to the *syn* product. Conversely, less acidic precatalysts favor the *E* Breslow intermediate geometry, leading to the *anti* product. These studies constituted a rare example of providing a rationale for stereoselectivity in NHC-catalyzed reactions.

In the same work, Rovis and Lee also examined an intramolecular Stetter reaction catalyzed by *chiral* NHC catalysts (reaction and protonated precatalyst shown in Figure 8). For this reaction, decreasing the gas-phase acidity of the chiral NHC precatalyst increased the desired *ee* of the reaction. Using the gas-phase results, the authors designed a precatalyst that they predicted would greatly improve the *ee*. This mesityl-substituted precatalyst indeed increased the *ee* of the solution-phase reaction from 73% to 90%. This was the first time that *gas-phase* properties of NHCs were used to design a catalyst which when used in a *solution-phase* Stetter reaction, improved the enantioselectivity of the *solution-phase* NHC-catalyzed reaction.

Another example involving gas-phase acidity and stabilized carbenes is the work of Bielawski and Lee (M. Chen et al., 2013). NHCs are more thermodynamically stable than traditional carbenes but are also more nucleophilic. The Bielawski group was interested in designing thermodynamically stable carbenes that might still display reactivity more commonly exhibited by reactive carbenes, such as insertion reactions. To achieve this, the Bielawski group developed a series of NHCs called "diamidocarbenes" (DACs, Figure 9) (Moerdyk & Bielawski, 2012, 2014; Moerdyk et al., 2016). DACs have been found to be more electrophilic than their NHC counterparts, due to the carbonyl groups, which pull electron density from the nitrogens. DACs are quite thermodynamically stable but also display reactivity more characteristic of classical carbenes, participating in C—H insertions, CO fixation, and activation of NH_3. Because DACs are more electrophilic than NHCs, they also might be more basic. To probe this hypothesis, Bielawski and Lee and coworkers measured and calculated the gas-phase PA of a series of DACs and NHCs (Figure 9) (M. Chen et al., 2013).

Because of the reactivity and high water sensitivity of DACs, protonated [DAC-H^+] was formed in the gas-phase through electrospray ionization of the hydrated DAC (Figure 9), in a modified quadrupole ion trap. The PA of a series of DACs was bracketed and compared to a series of NHC counterparts (Figure 9). Excepting the perfluoro substituted DAC, which was studied by the authors to examine steric effects, the PAs of the DACs were more basic than expected, and not too far from the NHC PAs (256–261 kcal/mol for the DACs, and 260–266 kcal/mol for the NHCs). The authors considered this unexpected, since the NHCs and DACs display very different reactivity. DFT calculations (B3LYP/6-31+G(d)) were used to calculate the

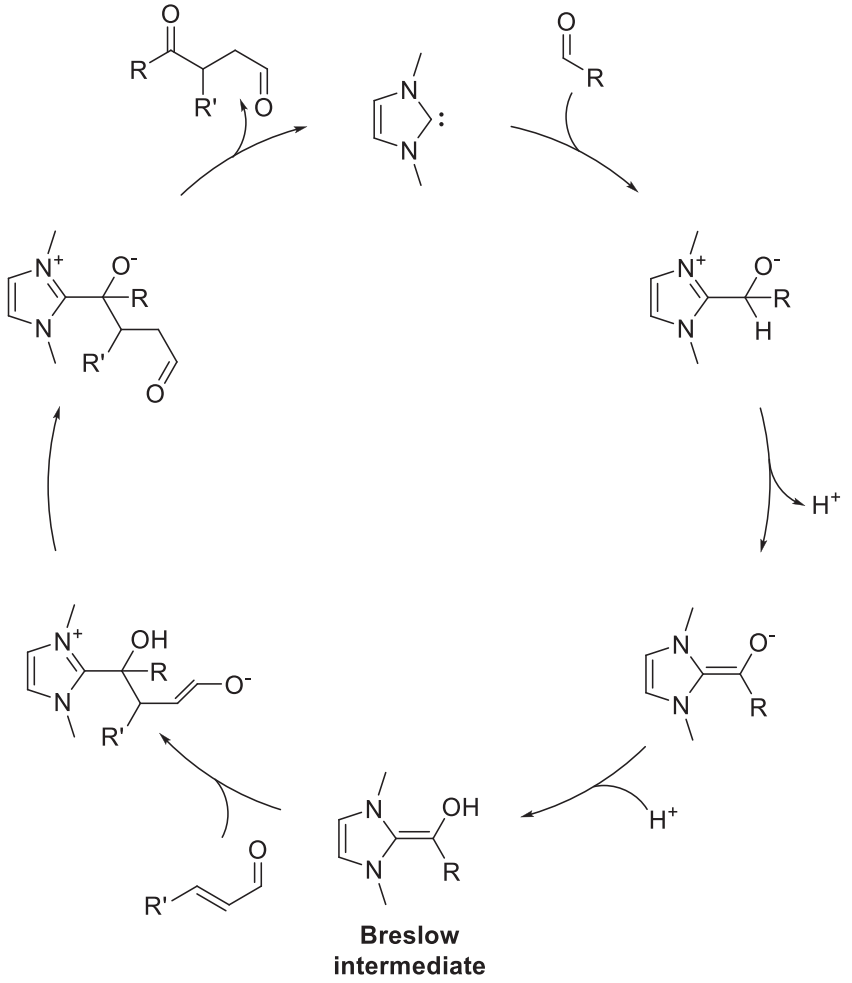

FIGURE 6 Catalytic cycle of the Stetter reaction

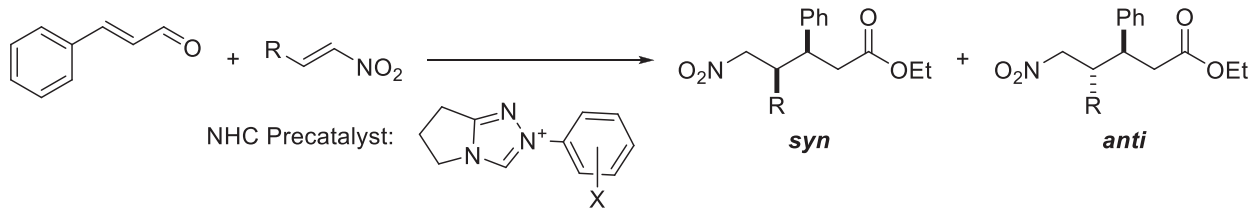

FIGURE 7 Stetter reaction with achiral catalyst studied by Rovis and Lee et al.

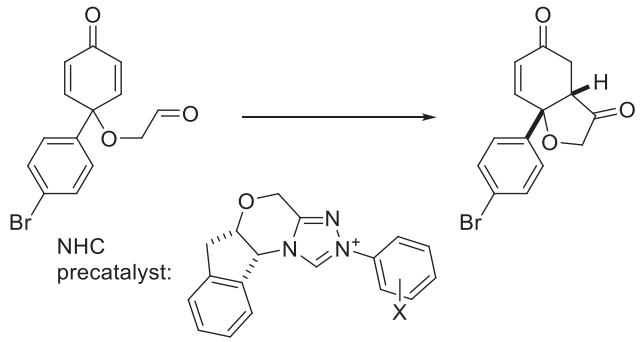

FIGURE 8 Intramolecular Stetter reaction with chiral catalyst studied by Rovis and Lee et al.

molecular orbitals of the DACs and NHCs. The HOMO-LUMO gap is much smaller for the DACs than the NHCs, which might explain why the DACs display more electrophilic characteristics. Additionally, Bielawski and Lee found that the DACs with *N*-aryl groups that have di-*ortho* alkyl substituents render the proton on the carbene site highly sterically hindered (Figure 9). This steric hindrance, combined with the bulkiness of the bases strong enough to deprotonate the protonated DAC, resulted in measured PA values that were higher than the calculated values. Additional DACs with less bulky *ortho* groups (perfluoro, tolyl, and *o*-anisidyl) were subsequently successfully measured (Figure 9).

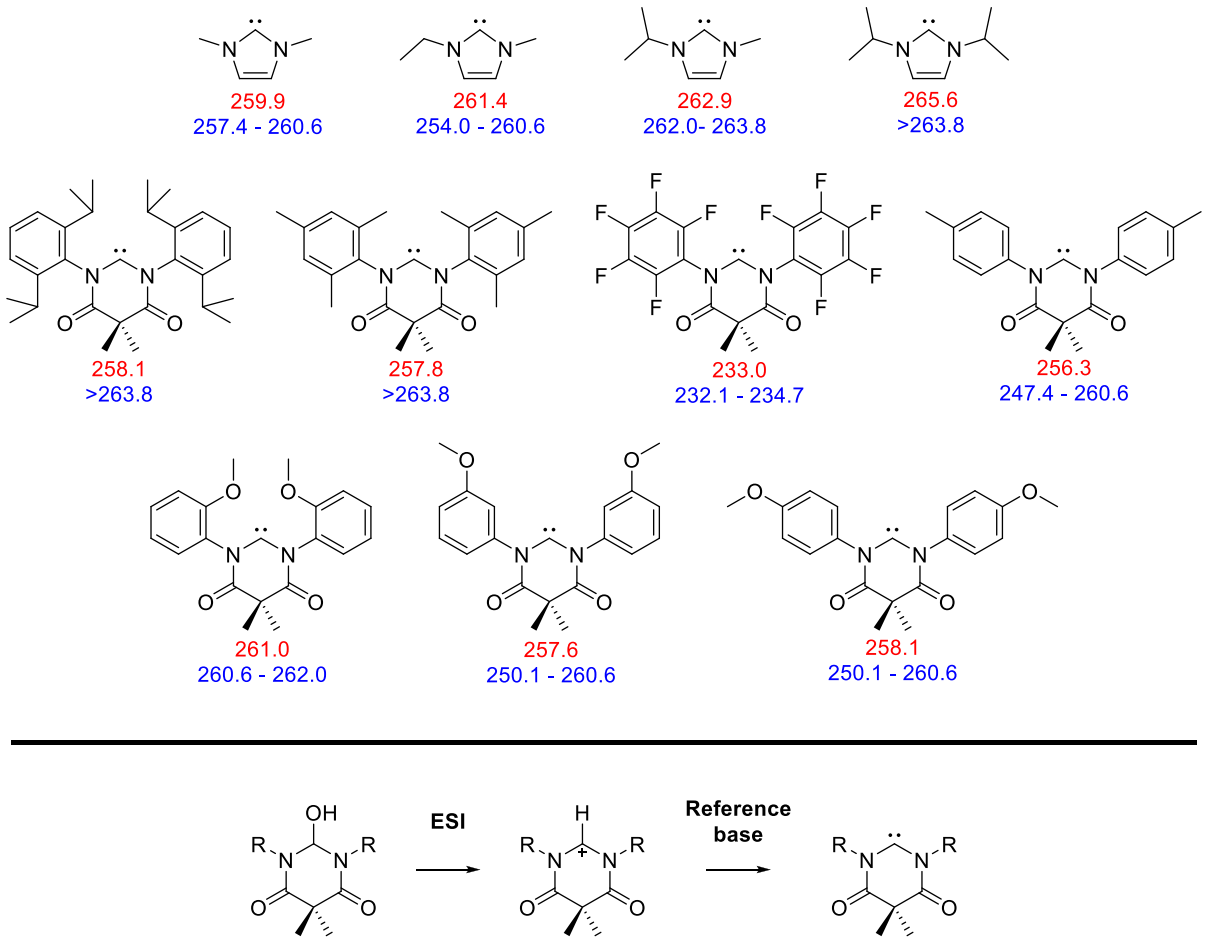

FIGURE 9 NHCs and DACS studied by Bielawski and Lee (M. Chen et al., 2013). Calculated PAs are in red and bracketed PAs are in blue. All energies are in kcal mol^{-1} At the bottom, the experimental scheme used. Calculations were performed using B3LYP/6-31 + G(d). DACS, diamidocarbenes; NHCs, *N*-Heterocyclic carbenes; PA, proton affinity. [Color figure can be viewed at wileyonlinelibrary.com]

2.2 | Alcohols and silanols

Silanols and silanediols have been recognized as potential catalysts in recent years (Chandrasekhar et al., 2004; Min et al., 2012; Pérez-Pérez et al., 2019). They have the ability to act as both a proton donor and proton acceptor. Silanols have been used as catalysts in polymerization reactions, Diels–Alder reactions, CO_2 fixation, and enantioselective aldol reactions (Chandrasekhar et al., 2004; Min et al., 2012; Pérez-Pérez et al., 2019; Tran et al., 2011). By comparison, large alcohols such as 1,1′-bi-2-naphthol (BINOL) and related compounds have uses in organocatalysis as well but are more often used as ligands in organometallic catalytic processes (Brunel, 2005; Huang et al., 2003).

Early work by Damrauer and coworkers (1991) established the influence of substituent effects on simple silanol systems. Using a flowing afterglow-selected ion flow tube (FA-SIFT), they found that silanols are more acidic than their alcohol counterparts. For example, SiH_3OH has a $\Delta G°_{acid}$ of 352 kcal mol^{-1} while CH_3OH has a $\Delta G°_{acid}$ of 374 kcal mol^{-1}. In addition to comparing relative acidities, they also found that alkyl groups in silanol systems lower gas-phase acidity, in contrast to their alcohol counterparts, where additional alkyl groups are known to increase acidity. This contrast was explained by alcohol acidity being largely influenced by polarizability over induction. For silanols, which have longer Si–O bonds, induction prevails. Since alkyl groups decrease acidity inductively, silanols with increased alkyl substitution are less acidic.

In 2011, Franz, Lee, and coworkers studied a series of silanols and silanediols, as well as their carbon counterparts, in an effort to uncover the inherent properties of silanols versus alcohols, in the context of the former as catalysts and hosts for molecular recognition (Figure 10) (Liu et al., 2011b). Silanediols are of particular interest because their carbon counterparts are not thermodynamically stable in solution—they dehydrate to form the more thermodynamically stable carbonyl species. Additionally, silanediols may act as double-point hydrogen-bonding catalysts, which may lead to multiple points of activation of reactants in catalytic cycles. Thus, the silanediols have potential as thermodynamically stable

hosts and catalysts. Franz, Lee, and coworkers found that while monosilanols are more acidic that their carbon counterpart alcohols (in agreement with the earlier Damrauer work), the studied silanediols are found to have acidities quite close to that of their theoretical carbon counterparts (as determined by DFT methods), and in some cases, the carbon diols are more acidic that the silanediols. These trends are proposed to be due to two factors—polarizability and internal hydrogen bonding. Highly polarizable groups, such as *tert*-butyl and phenyl groups, enhance the acidity more in the carbon analogues than in the silicon analogues. In addition, deprotonation of the diols results in an anionic oxide group that can hydrogen bond with the nearby "OH" moiety. This hydrogen bond is significantly longer for the deprotonated silanediols than the analogous carbon diols; therefore, the hydrogen bond stabilizes the deprotonated carbon diol more, greatly increasing the acidity of the neutral conjugated acid.

The diols were also examined in the context of hydrogen bonding and catalysis. Calculations showed that most of the silanediol structures have intramolecular H-O distances greater than 3.0 Å, which supports these species serving as double- (not single-) point hydrogen bonding activators, like BINOL. Comparing the determined gas-phase acidities with yields of a catalytic Diels–Alder reaction of methacrolein and Rawal's diene in toluene, the authors found that the more acidic the silanol within its class (monosilanol, silanediol, and disiloxanediol), the better the catalyst (Kozmin & Rawal, 1997). The carbon analogues of each of the silanol catalysts showed less catalytic activity as well.

2.3 | Pyridine *N*-oxides

Organocatalysts derived from pyridine *N*-oxide moieties have been used as successful Lewis base catalysts for the addition reaction of allyltrichlorosilane and aldehydes (Figure 11) (Wrzeszcz & Siedlecka, 2020).

These catalysts work through the activation of the carbon-silane bond by oxygen; this activation is facile due to the polarized nitrogen–oxygen bond of the *N*-oxide, as well as oxygen's affinity for silicon, allowing the oxygen of the

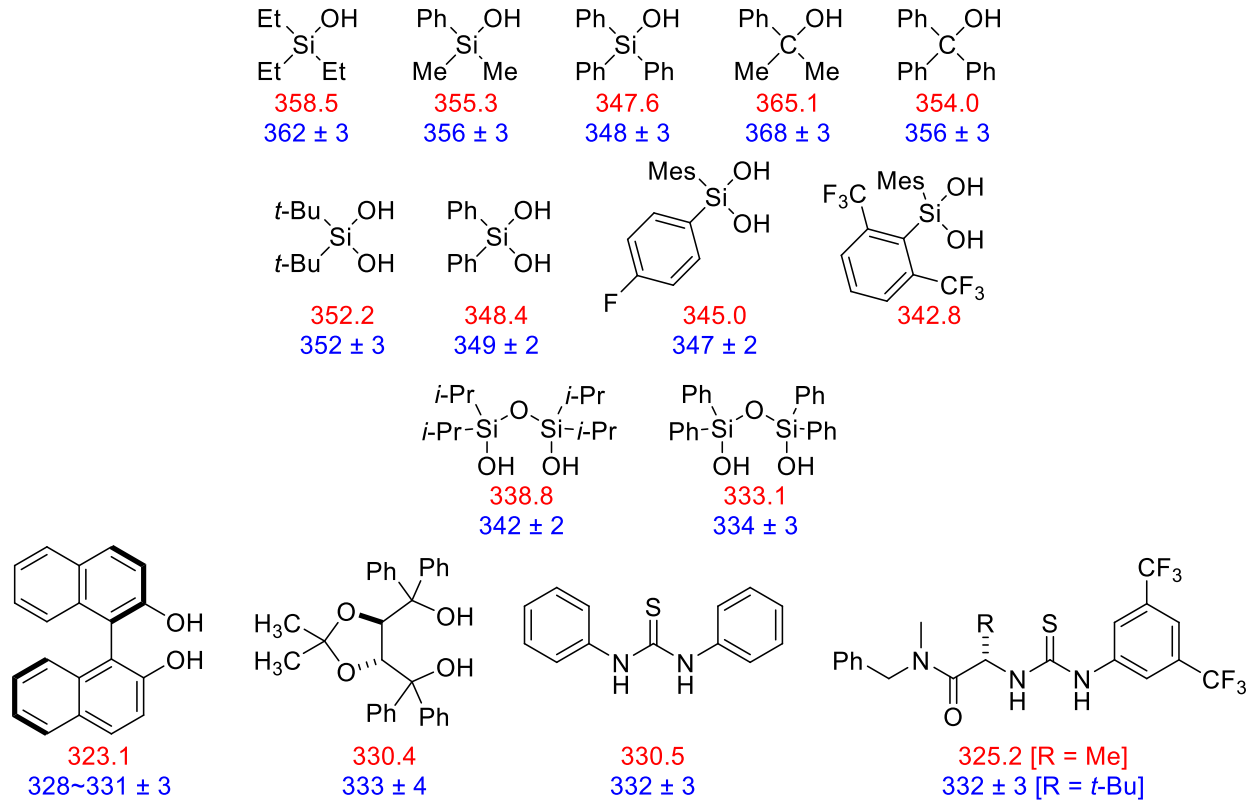

FIGURE 10 Silanols, silanediols, and dual hydrogen bonding catalysts studied by Lee and Franz et al. Calculated PAs are in red and bracketed PAs are in blue. All energies are in kcal mol^{-1}. PA, proton affinity. [Color figure can be viewed at wileyonlinelibrary.com]

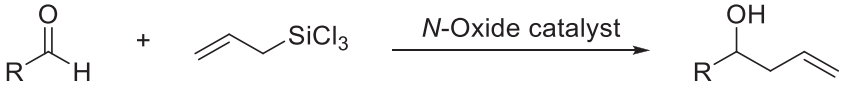

FIGURE 11 Reaction catalyzed by *N*-oxide catalysts

N-oxide to act as a Lewis base (Malkov, Stončius, et al., 2013). This transformation is a subset of Lewis base-catalyzed Sakurai–Hosomi–Denmark type reactions (Lade et al., 2017).

A series of chiral *N*-oxide catalysts based on C_2-symmetric bipyridine scaffolds have been developed by the Kotora and Kočovský labs, and have been shown to be effective at catalyzing enantioselective allylation of aromatic aldehydes with allyltrichlorosilanes (Figure 12) (Malkov, Barłóg, et al., 2011; Malkov, Bell, et al., 2005; Malkov, Bell, et al., 2003; Malkov, Dufková, et al., 2003; Malkov, Ramírez-López, et al., 2008; Malkov, Stončius, 2013). In 2014, the Roithova lab studied the PAs of these *N*-oxide catalysts (Váňa et al., 2014). Using a Thermo-Finnigan TSQ Classic mass spectrometer, the authors determined the PAs of the catalysts using a combination of experimental (extended Cooks kinetic method), and computational (DFT calculations for the determination of theoretical PA and pK_a values) methods. In the gas-phase, all of the bases were found to have PAs in the range of 248–255 kcal mol^{-1}, placing them well within what would be considered to be "superbase" range in the gas-phase (Kaljurand et al., 2007; Leito et al., 2015; Puleo et al., 2021). It was found computationally that when these catalysts are protonated, there is a large geometrical change in the dihedral angles between the tethered pyridine rings, due to the dual proton acceptor groups both participating in the binding of the acidic proton (those being the *N*-oxide groups, or one *N*-oxide group and one methoxy group) (Figure 13). The authors also found large deviations from linearity in the Cooks extended method workup, particularly at very low collision energies, indicating significant entropy effects.

The authors found no correlation between the change in the dihedral angle of the pyridines and the PA of each catalyst. Additionally, it was found that the most highly aromatic species had the lowest PAs, while replacement of one of the phenyl groups with cyclohexane increased the PA. This is indicative that electronic effects play a much larger role in the PA of the catalysts than geometric effects. Another feature is that the catalysts are not very basic in ethanol, with pK_as around 0.8. In the gas-phase, however, the catalysts are quite formidable bases, with proton affinities all greater than 248 kcal mol^{-1}. Thus, relatively speaking, the catalysts are much more basic in the gas-phase. Finally, the authors propose that due to high basicity, these compounds could

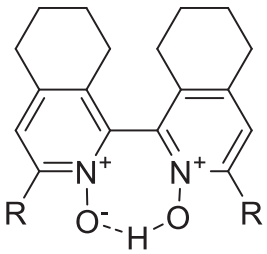

FIGURE 13 Example of dual proton donor–acceptor participation in *N*-oxide catalysts

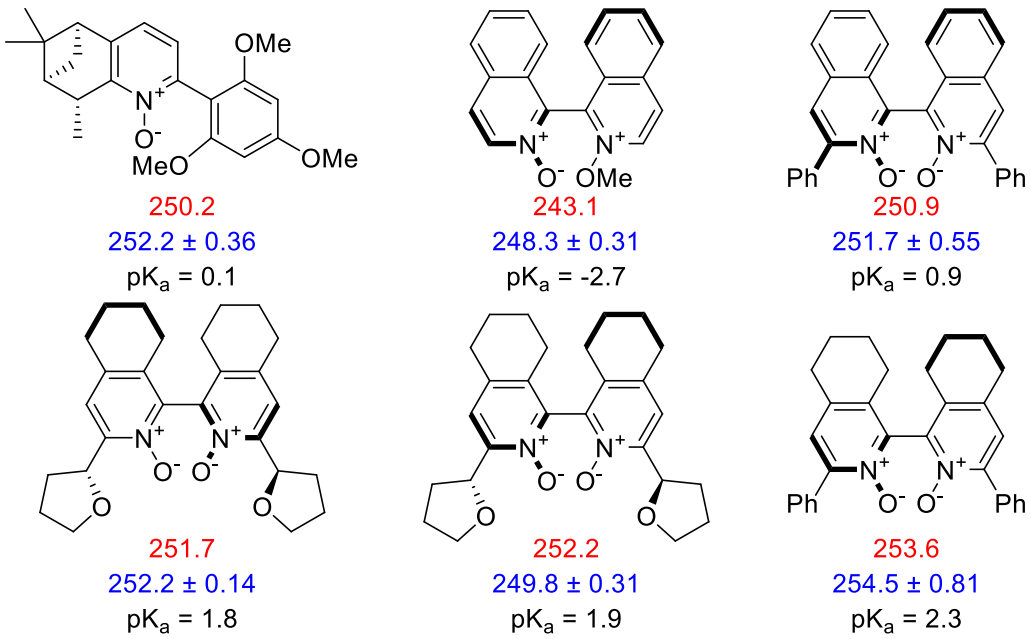

FIGURE 12 *N*-oxide bases studied by the Roithova group. All calculations were run using B3LYP-D3/def2-TZVP. Calculated PAs in red, experimental PA values in blue. pK_a values calculated using COSMO-RS solvation energies. PA, proton affinity. [Color figure can be viewed at wileyonlinelibrary.com]

potentially be useful as matrices for matrix-assisted ionization/laser desorption (MAILD) MS metabolomics studies (Miura et al., 2012; Ren et al., 2018).

2.4 | Guanidines and 2-iminoimidazolines

Over the past few decades, guanidines, guanidinium ions, and related compounds have been studied as "superbases," which act as organocatalysts in many reactions. They have been particularly effective for asymmetric catalysis, owing in part to their ability to act as both Brønsted acid–base catalysts and Lewis bases, as well as their ability to act as hydrogen-bond donors and acceptors (Kee & Tan, 2016; Selig, 2013).

In an effort to understand the role that intramolecular hydrogen bonds play in the basicity of guanidines, Schröder, Schwartz, and coworkers determined the gas-phase PAs of a series of guanidines, many of which contain heteroalkyl side chains (Figure 14) (Glasovac et al., 2008). The Cooks kinetic method was used for the PA measurements, and calculations using MP2 and B3LYP were also conducted. Particular emphasis was placed on guanidines containing 3-(*N*,*N*-dimethylamino)propyl- or 3-methoxypropyl substituents, as these should be strong hydrogen-bond acceptors. They chose *N*,*N*′,*N*″-tripropylguanidine as a reference compound, due to its having the same through-bond inductive effects as in a guanidine core, but without the ability to form intramolecular hydrogen bonds in either neutral or protonated forms (Figure 14). The ability of the heteroalkyl guanidines to form intramolecular hydrogen bonds was found to correlate with increased PA. Generally, the calculated and experimental PAs were in agreement, but it was important to consider entropic effects, which can be an issue with the Cooks kinetic method (Bouchoux et al., 2004; Cooks & Wong, 1998). The authors also noted that obtaining an accurate PA of the most basic guanidines was hindered by the lack of suitably basic reference bases.

In 2012, Polyakova, Kunetskiy, and Schröder investigated the PAs of 2-iminoimidazolines containing bulky *N*-alkyl-substituents (Figure 15) (Polyakova et al., 2012). The bulky *N*-alkyl substituents are expected to increase PA through donation, as well as make the compounds more lipophilic. The high lipophilicity allows for solvation in nonpolar organic solvents, which further increases the applicability of guanidines as organocatalysts in nonpolar phases. These imidazole-2-ylidenes also can be thought of as carbene analogs of iminophosphoranes, which are well-known superbases. The species are additionally of interest as potential ligands for metal complexes used in catalytic reactions.

The Cooks kinetic method was utilized to measure PAs, and density functional calculations were also conducted. Reference bases 1,8-diazabicyclo[5.4.0]undec-7-ene (DBU), 1,5,7-triazabicyclo[4.4.0]dec-5-ene (TBD), and 7-methyl-1,5,7-triazabicyclo[4.4.0]dec-5-ene (MTBD) were used. All of the 2-iminoimidazoles were found to be more basic than the most basic reference, MTBD (PA = 254.0 kcal mol^{-1}). The authors then used

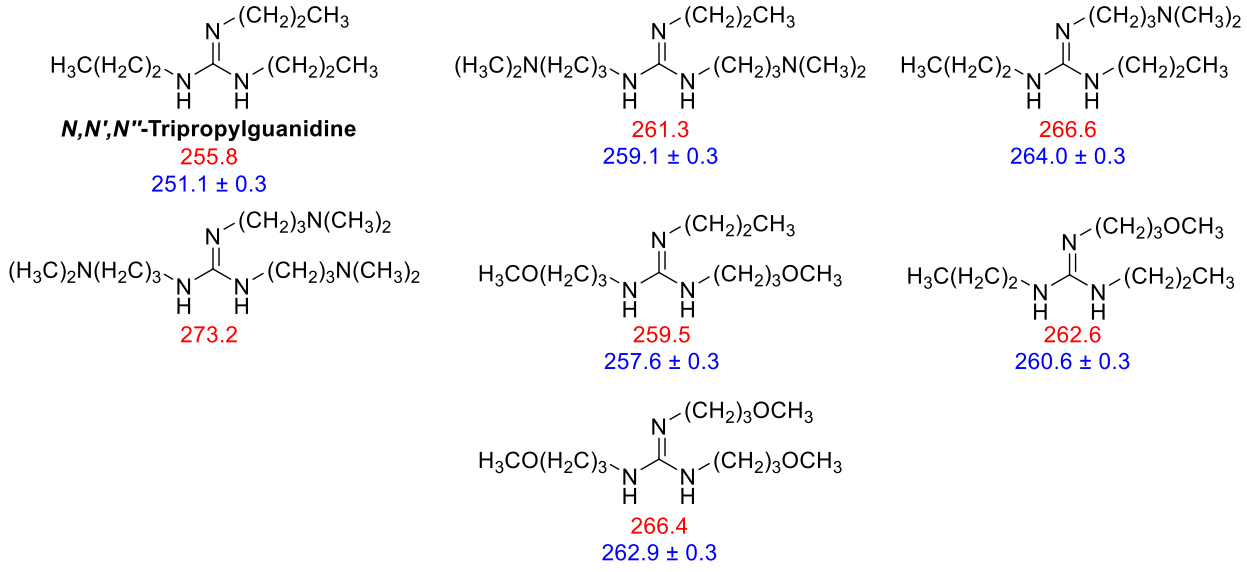

FIGURE 14 PAs of substituted guanidines determined by the Schwarz lab. Calculations performed at the DFT theory level B3LYP/6-311+G(2df,p)//B3LYP/6-31G(d). Calculated values are in red, with experimental values in blue. PA, proton affinity. [Color figure can be viewed at wileyonlinelibrary.com]

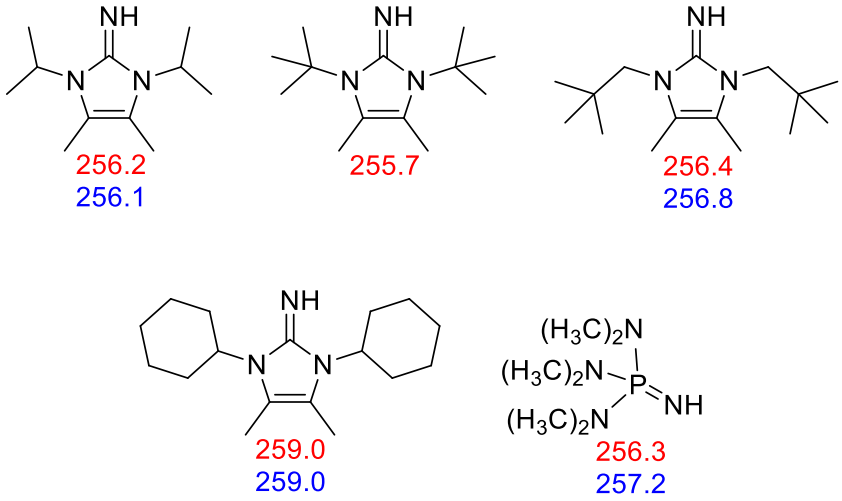

FIGURE 15 2-Iminoimidazolines and iminophosphorane studied by Schröder et al. Calculations performed using B3LYP/6-311+G (d,p). Calculated values are in red with experimental values in blue. [Color figure can be viewed at wileyonlinelibrary.com]

mixed proton-bound dimers containing two iminoimidazole units to further determine relative PAs. The PAs were found to be in the range of 256–260 kcal mol^{-1}, with the cyclohexyl substituted iminoimidazoline being the most basic. The authors also note that the substrate with *tert*-butyl substituents may have an erroneously measured PA, due to steric hindrance issues. Calculations support this hypothesis. Generally, the experimental and calculated PAs are well correlated. Furthermore, protonation did not appear to incur any significant conformational changes. The authors were also able to measure the PA of the iminophosphorane $(Me_2N_3)P{=}NH$, using the newly measured 2-iminoimidazolines as references. The phosphorane was found to be slightly more basic than all the other studied iminoimidazolines, with the exception of the cyclohexyl-substituted species. The measured PA is also in agreement with a prior theoretical publication, providing a nice benchmark for the experimental method.

3 | BIO-ORGANIC CATALYSIS

Enzymes are often therapeutic targets, as key biological pathways can be influenced by modifying or inhibiting the reactions that the enzymes catalyze. Although the gas-phase may seem like an unlikely medium for examining biological reactions, many enzymes actually have a fairly hydrophobic active site, such that the gas-phase can provide a reasonable model (Bennett et al., 2006; Kiruba et al., 2016; Kurinovich & Lee, 2000, 2002; Kurinovich et al., 2002; Michelson, Chen, et al., 2012; Michelson, Rozenberg, et al., 2012; Simonson & Brooks, 1996; Zhachkina & Lee, 2009).

In the next portion of this review, we focus on gas-phase mass spectrometric work that has been conducted to reveal insights into biological catalysis.

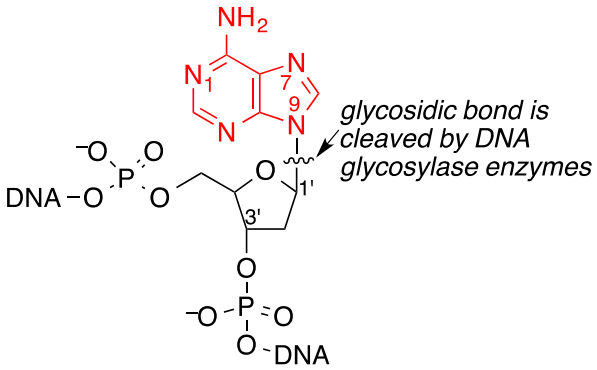

FIGURE 16 Glycosidic bond cleaved by DNA glycosylases [Color figure can be viewed at wileyonlinelibrary.com]

3.1 | Glycosylases

Glycosylases are enzymes that catalyze the cleavage of the *N*-glycosidic bond in DNA to release damaged nucleobases (Figure 16). Gas-phase methods have been used to examine various substrates for these enzymes; we focus on a few examples.

3.2 | Uracil DNA glycosylase

The integrity of DNA is essential for normal cell function. DNA is, however, subject to constant assault, by both endogenous and exogenous agents (Berti & McCann, 2006; Stivers & Jiang, 2003). Such damage is deleterious to the genome, and is associated with carcinogenesis and cell death.

Uracil is a naturally occurring RNA base but can arise in DNA through either misincorporation or cytosine deamination. Uracil DNA glycosylase (UDG) excises uracil from DNA (Figure 17).

To lend insight into the UDG mechanism, Kurinovich and Lee examined uracil in the gas-phase (Kurinovich & Lee, 2000, 2002; Kurinovich et al., 2002). At the time of their study, the proposed mechanism involved nucleophilic attack by activated water on the C1′. In this scenario, deprotonated uracil is the leaving group (Figure 17). Kurinovich and Lee asked the question, how good of a leaving group is uracil deprotonated at N1 (hereafter referred to as the "$N1^-$ anion")? Since leaving group ability is often related to acidity (the conjugate bases of more acidic groups are better leaving groups), then for uracil $N1^-$ to be a good leaving group, uracil must be quite acidic at the N1-H position. Lee and Kurinovich were further intrigued by the gas-phase acidity at the N1-H, (Kurinovich & Lee, 2000) because in solution, both the N1-H and N3-H protons have the same pK_a (Kimura et al., 1997; Nakanishi et al., 1961). Thus, this study was motivated by the UDG mechanism, but also by a desire to uncover the intrinsic, gas-phase properties of the biological substrate uracil.

The authors found that the N1-H of uracil *in vacuo* is very acidic—comparable to hydrochloric acid ($\Delta H_{acid} = 333 \pm 4$ kcal/mol). Furthermore, the N3-H proton is roughly 14 kcal/mol *less* acidic than the N1-H, despite the two protons having similar acidity in water (Kurinovich & Lee, 2000). These results showed how a nonpolar environment can change relative acidities. Because enzyme active sites are often quite nonpolar, such gas-phase studies could have biological relevance (Bennett et al., 2006; Kiruba et al., 2016; Kurinovich & Lee, 2000, 2002; Kurinovich et al., 2002; Michelson, Chen, et al., 2012; Michelson, Rozenberg, et al., 2012; Simonson & Brooks, 1996; Zhachkina & Lee, 2009). Furthermore, in a biological sense, the results indicate that in hydrophobic, nonaqueous environments, the deprotonated uracil anion is a relatively good "leaving group." Therefore, Kurinovich and Lee postulated that uracil DNA glycosylase might provide a hydrophobic environment that would enhance the relative leaving group ability of uracil over that of other undamaged bases. Later enzyme studies confirmed that the deprotonated uracil anion (as opposed to a pre-protonated neutral species) was in fact the product of uracil DNA glycosylase cleavage, as proposed from gas-phase studies (Berti & McCann, 2006; Dinner et al., 2001; Dong et al., 2000; Drohat & Stivers, 2000a, 2000b; Jiang et al., 2002; Werner & Stivers, 2000).

Because of the importance of leaving group ability in the UDGase mechanism, Zhachkina and Lee explored this topic further in 2009 (Zhachkina & Lee, 2009). Hydrochloric acid and uracil N1-H have similar acidities, but do they have similar leaving group abilities? While acidity of a compound and the leaving group ability of its conjugate base are often related, the former is still a thermochemical feature, while the latter is kinetic. To lend insight into this question, Zhachkina and Lee studied the leaving group abilities of chloride versus 3-methyluracil, through reaction with a series of nucleophiles Nu^-, using gas-phase experimentation and computation (Figure 18, Reactions 1 and 2) (Zhachkina & Lee, 2009). It was found that despite their comparable gas-phase acidities, the leaving group abilities are different, with chloride being a slightly better leaving group than N1-deprotonated 3-methyluracil. The authors also compared the leaving group ability of N1-deprotonated 3-methyluracil and N1-deprotonated 3-methylthymine (Figure 18, Reactions 2 and 3). They discovered that the deprotonated methyluracil is a slightly better leaving group than deprotonated 3-methylthymine, lending support to the hypothesis that UDGase cleaves uracil more readily than thymine from DNA because of differential reactivity. That is, the difference in reactivity uncovered by Zhachkina and Lee may be a factor in how UDG selectively cleaves uracil, and not thymine from DNA.

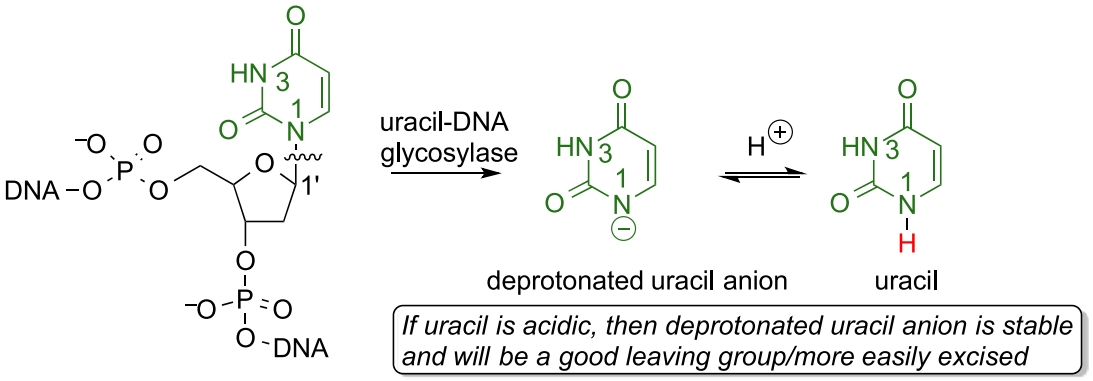

FIGURE 17 Uracil-DNA glycosylase reaction [Color figure can be viewed at wileyonlinelibrary.com]

3.3 | Alkyladenine DNA glycosylase and 3-methyladenine DNA glycosylase II

Alkylation is a major source of DNA damage. To counteract the toxic and mutagenic effects of environmental and endogenous alkylating agents, distinct DNA alkylation repair mechanisms have evolved (Berti & McCann, 2006; Sedgwick, 2004; Stivers & Jiang, 2003). The excision of certain damaged purine bases is catalyzed by alkyladenine DNA glycosylase (AAG) in humans, and 3-methyladenine DNA glycosylase II (AlkA) in *Escherichia coli*. Both of these enzymes are "broadly specific," cleaving a wide range of damaged bases while leaving adenine and guanine untouched. As with uracil DNA glycosylase, the mechanism cleaves the N9-C1′ ribose bond, such that the leaving group is the conjugate base of the purine (Figure 19). Several mass spectrometric studies by Lee and coworkers have focused on lending insight into this enzyme mechanism (Liu, Xu, et al., 2008; Michelson, Chen, et al., 2012; Sharma & Lee, 2002; Zhachkina et al., 2009).

Early work established that 3-methyladenine, which is a lesion that both AlkA and AAG excise, is unusually acidic in the gas-phase, much more so than the naturally occurring nucleobases adenine and guanine (Figure 20, Table 1) (Sharma & Lee, 2002). This was followed by mass spectrometric studies showing that hypoxanthine and 1,N^6-ethenoadenine, also lesions removed by AlkA and AAG, are more acidic than adenine and guanine (Table 1) (Liu, Xu, et al., 2008; Sun & Lee, 2007). More significantly, the difference in acidity between the damaged and normal nucleobases is enhanced in the gas-phase. These three studies established that enzymes such as AlkA and AAG, which cleave a wide range of damaged bases, may be utilizing a nonpolar active site to differentiate the lesions. The

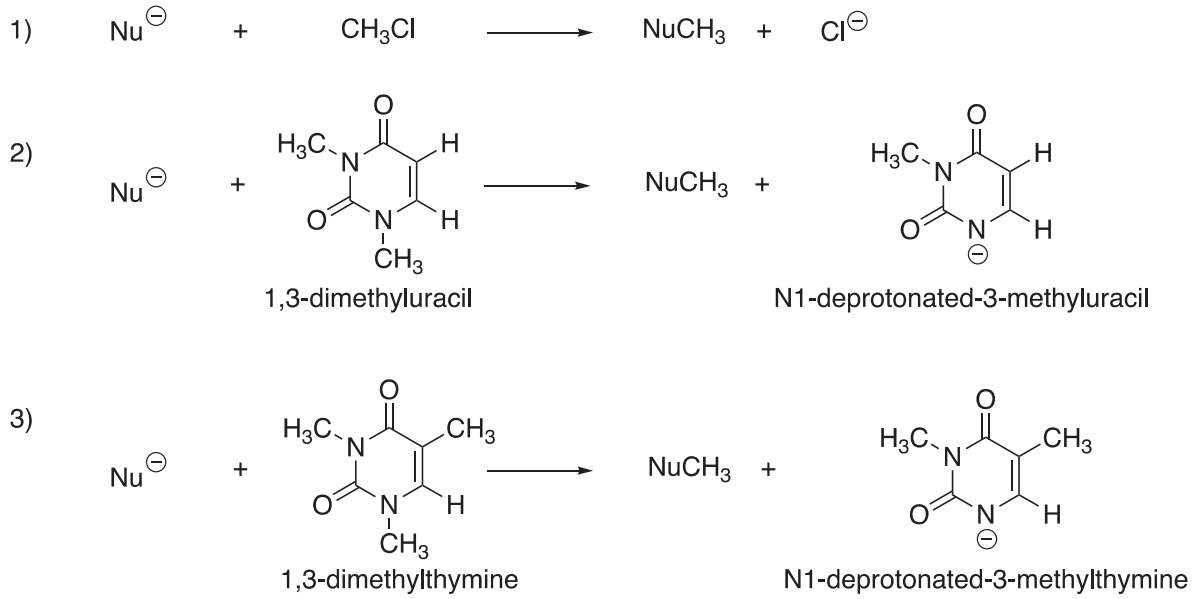

FIGURE 18 Leaving group ability studies by Zhachkina and Lee

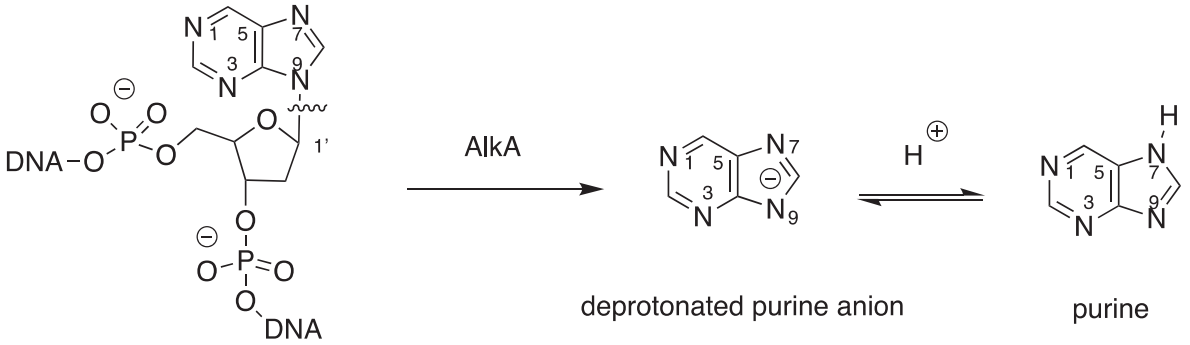

FIGURE 19 Bond scission by AlkA. AlkA, 3-methyladenine DNA glycosylase II.

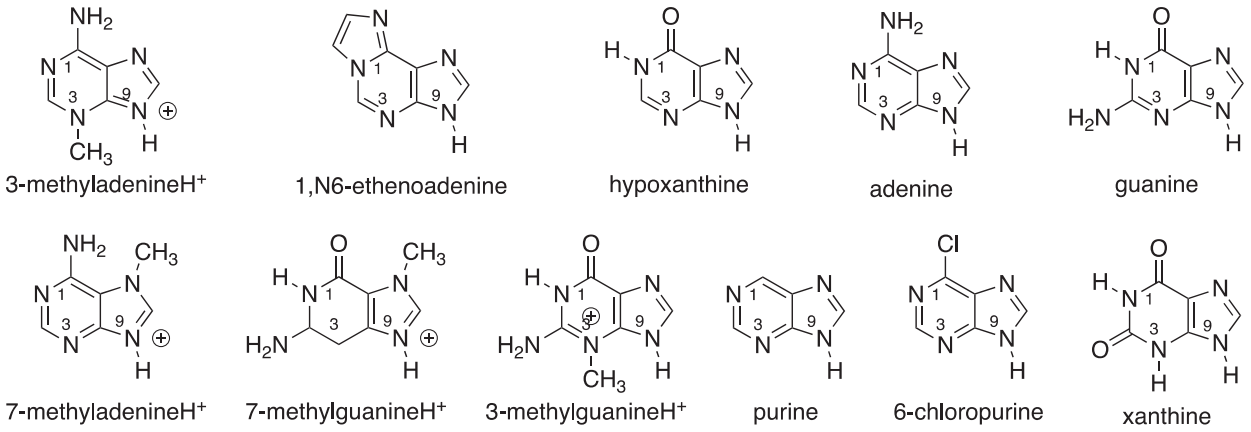

FIGURE 20 AlkA and AAG substrates. AlkA, 3-methyladenine DNA glycosylase II.

TABLE 1 Calculated and experimental data for AlkA and AAG substrates (Liu, Xu, et al., 2008; Michelson, Chen, et al., 2012; Sharma & Lee, 2002; Zhachkina et al., 2009).

	Substrate	Calculated value[a]	Experimental value[b]
ΔH_{acid}[c]	7-Methyladenine	342.2	344 (344)
	7-Methylguanine	335.6	337 (337)
	3-Methyladenine	346.8	347
	3-Methylguanine	328.6	N/A
	Purine	329.8	333 (332)
	6-Chloropurine	322.8	<328
	Xanthine	324.7	323–328 (327)
	1,N^6-ethenoadenine	330.7	332
	Hypoxanthine	331.3	332
	Adenine	334.8	333 (335)
	Guanine	334.4	(335)
PA[c]	7-Methyladenine	234.7	234 (234)
	7-Methylguanine	231.4	231 (232)
	3-Methyladenine	234.5	233
	3-Methylguanine	231.8	N/A
	Purine	219.2	220 (221)
	6-Chloropurine	212.5	214
	Xanthine	205.2	211 (212)
	1,N^6-ethenoadenine	232.6	232 (233)
	Hypoxanthine	218.8	217.5–220.2 (222)
	Adenine	223.7	224 (225)
	Guanine	227.4	(227)

[a]Calculated at 298 K, using B3LYP/6-31+G(d).

[b]Nonparenthetical experimental value is from bracketing measurement; Cooks kinetic method value is in parentheses. Error is ±2–4 kcal/mol.

[c]All values are reported as enthalpies, in kcal/mol.

damaged bases are more acidic, and therefore their conjugate base anions would be better leaving groups, and the enzymes may provide a hydrophobic site to take advantage of the enhanced acidity for the damaged bases. A follow-up gas-phase study of 9-mer DNA duplexes containing hypoxanthine was inconclusive on whether the gas-phase changed duplex stability in such a way as to help hypoxanthine excision, as the stability was very sequence-dependent (Sun & Lee, 2010). A more comprehensive gas-phase study on a wide range of AlkA substrates (7-methyladenine, 7-methylguanine, 3-methyladenine, 3-methylguanine, purine, 6-chloropurine and xanthine, data in Table 1) found a clear correlation between gas-phase acidity and AlkA excision rates, lending further support to a mechanism in which the enzyme provides a nonpolar, nonspecific active site (Michelson, Chen, et al., 2012). Nucleobase cleavage is thus dependent on the intrinsic *N*-glycosidic bond stability; the hydrophobic environment works to enhance the differences between damaged and normal nucleobase reactivity.

3.4 | MutY

Another enzyme for which gas-phase studies have lent insight is the adenine glycosylase MutY. Oxidative damage of DNA is extremely prevalent, and one of the most common lesions results from the oxidation of guanine, to form 8-oxo-7,8-dihydroguanine (OG). During DNA replication, the polymerase will insert an adenine (A) opposite OG, as the OG:A pair is preferred. MutY is an *Escherichia coli* enzyme that cleaves adenine when adenine is mispaired to OG. The enzyme is remarkably specific, not touching adenine in A:T base pairs.

Lee and David and coworkers explored a series of synthetic adenine analogs, which were modified in specific ways, to target the role that various moieties on the adenine might play in MutY recognition and excision (Figure 21) (Michelson, Rozenberg, et al., 2012). 7-Deazaadenine (Z), 3-deazaadenine (Z3), and 1-deazaadenine (Z1) are missing the nitrogen at the N7, N3, and N1 positions, respectively (as compared to adenine). The next three substrates in Figure 21 are all nonpolar isosteres of adenine (B, Q, M). Gas-phase mass spectrometric studies were used to measure the PA and acidity of these adenine analogs, both to characterize them and to benchmark calculations (Table 2). Once a computational level was found that matched the experimentally derived values, the authors used that

TABLE 2 Calculated and experimental data for MutY substrates (Michelson, Rozenberg, et al., 2012)

	Substrate	Calculated value[a]	Experimental value[b]
ΔH_{acid}[c]	Z	343.5	347
	Z3	335.3	337
	Z1	340.6	(341)
	Q	338.4	341
	M	347.9	(349)
	B	339.4	343
	adenine	334.8	333 (335)
PA[c]	Z	228.4	228
	Z3	233.2	233
	Z1	230.0	(232)
	Q	223.0	225.5-228.0
	M	215.7	N/A
	B	228.2	228
	adenine	223.7	224 (225)

[a]Calculated at 298 K, using B3LYP/6-31+G(d).

[b]Non-parenthetical experimental value is from bracketing measurement; Cooks kinetic method value is in parentheses. Error is ±3–4 kcal/mol.

[c]All values are reported as enthalpies, in kcal/mol.

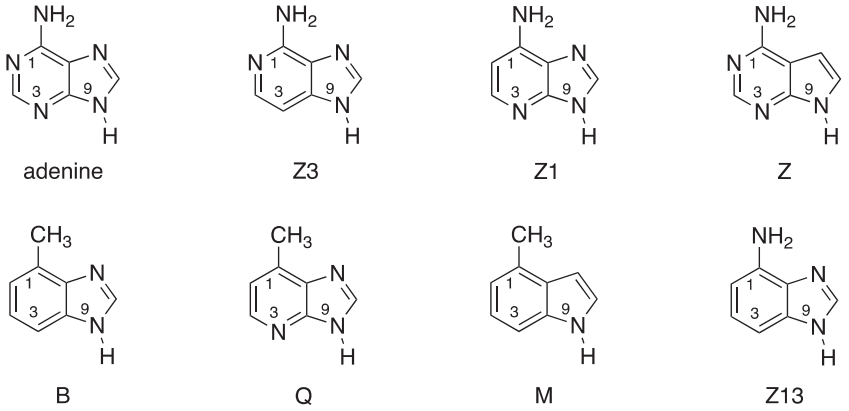

FIGURE 21 Synthetic adenine analogs for MutY study

method to explore the MutY mechanism further. Comparison of predicted excision rates for different mechanisms as predicted by calculations, with actual MutY excision data, point to a mechanism where adenine is protonated at N7, and a hydrogen bond is formed at N3, to enhance cleavage. Lee and David also explored the nonenzymatic acid-catalyzed depurination of oligonucleotides containing the adenine analogs. Using their gas-phase methods, they established that depurination in the absence of enzyme most likely takes place via protonation of the most basic site of the adenine analog, followed by glycosidic bond breakage. Last, based on the mass spectrometric and computational results, the authors made a prediction that the adenine analog 1,3-deazaadenine (Figure 21, Z13) would be cleaved more slowly than B, but faster than Z and M, by MutY. In acidic solution, the prediction is that Z13 would undergo depurination more quickly than adenine.

3.5 | Orotidine 5′-monophosphate decarboxylase

The decarboxylation of orotidine 5′-monophosphate to form uridine 5′-monophosphate is a key step in the *de novo* biosynthesis of pyrimidine nucleobases. The reaction is catalyzed by orotidine 5′-monophosphate decarboxylase (ODCase), which is one of the most proficient enzymes known (Figure 22) (Radzicka & Wolfenden, 1995). The reaction is of interest because decarboxylation initially results in a vinylic anion, which should not be particularly stable, although it does have a favorable carbene resonance structure (Figure 22). Kurinovich and Lee examined uracil and a series of uracil derivatives in the gas-phase and established that the C6-H position in uracil and derivatives is actually quite acidic in the gas-phase, comparable to acetaldehyde (Table 3) (Kurinovich & Lee, 2000, 2002). Subsequent studies of adenine and derivatives by Sharma and Lee showed a pattern of enhanced vinylic C–H acidities when adjacent to an N-R group (Table 4, C8-H and C2-H acidities in the 370 kcal/mol range) (Sharma & Lee, 2004). These studies support the possibility that ODCase may also provide a somewhat hydrophobic environment, where decarboxylation produces a surprisingly stable anion.

3.6 | Formamidopyrimidine glycosylase (Fpg)

Fpg, also called MutM, catalyzes the removal of OG from OG:C base pairs in *Escherichia coli*. Like other glycosylases, it also cleaves a wide range of nucleobases in addition OG, including 8-oxoadenine (OA), 8-oxoinosine (OI), and 8-oxonebularine (ON), formamidopyrimidine-guanine (FapyG), 5-hydroxyuracil (OHU), and 5,6-dihydrothymine (DHT) (Figure 23). Mass spectrometric experiments were used to measure the acidity and PA of some of these substrates (Table 5), which provided new data and also benchmarked the attendant computational method (Kiruba et al., 2016). Calculations were used to explore the Fpg mechanism; as this review focuses on

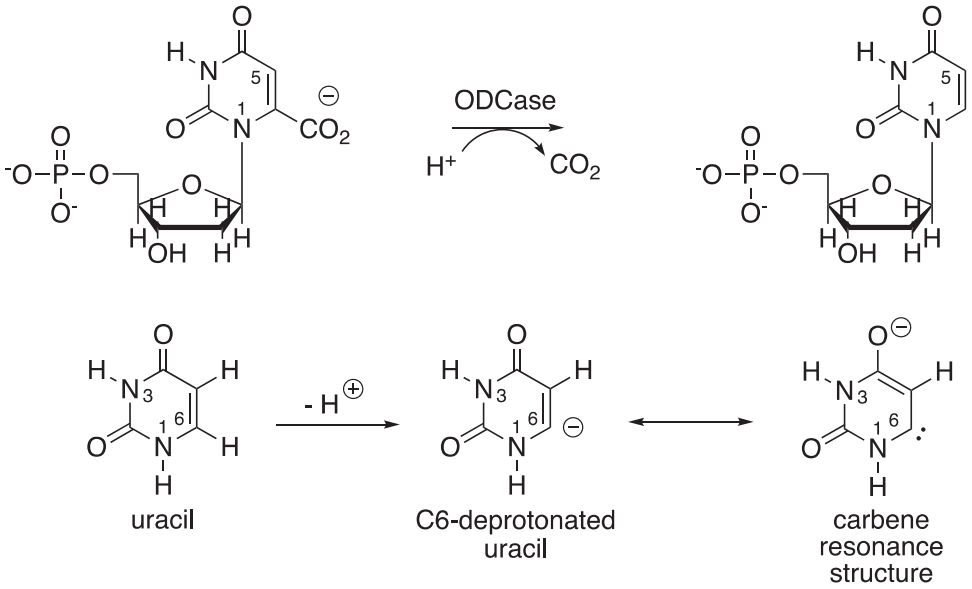

FIGURE 22 Reaction catalyzed by ODCase and substrates studied

TABLE 3 Summary of experimental and calculated gas-phase acidities of the different sites of uracil and alkylated-uracils, in kcal/mol (Kurinovich & Lee, 2000, 2002)

Structure[a]	N1	N3	C5	C6
Uracil	333 ± 4 (329.0)	347 ± 4 (342.6)	NM (376.1)	NM (361.5)
1-Methyluracil	NA	348 ± 3 (343.8)	NM (377.3)	363 ± 3 (362.9)
3-Methyluracil	333 ± 2 (331.3)	NA	NM (378.4)	363 ± 3 (363.5)
6-Methyluracil	331 ± 3 (330.5)	352 ± 5 (344.1)	NM (377.8)	NA
5,6-Dimethyluracil	333 ± 2 (331.7)	349 ± 3 (344.6)	NA	NA
1,3-Dimethyluracil	NA	NA	384 ± 3 (378.7)	369 ± 2 (365.6)

Abbreviations: NA, "not applicable" (site is alkylated so there is no proton to remove for acidity measurement); NM, not measured.

[a]Nonparenthetical values are experimental data; values in parentheses are calculated at 298 K, using B3LYP/6-31+G*. All values are enthalpies, in kcal/mol.

TABLE 4 Summary of experimental and calculated gas-phase acidities of various sites of adenine and alkylated adenines, in kcal/mol (Sharma & Lee, 2002, 2004)

Structure[a]	N9	N10	C8	C2
Adenine	333 ± 2 (334.8)	352 ± 4 (353.5)	NM (373.1)	NM (399.0)
9-Ethyladenine	NA	352 ± 4 (354.4)	374 ± 2 (373.8)	NM (399.5)
3-Methyladenine	NA	347 ± 4 (346.8)	NM (399.9)	370 ± 3 (368.8)
1-Methyladenine	331 ± 2 (334.3)	NA	NM (375.6)	NM (374.6)
N,*N*-dimethyladenine	333 ± 2 (335.5)	NA	NM (373.4)	NM (399.6)

Abbreviations: NA, "not applicable" (site is alkylated so there is no proton to remove for acidity measurement); NM, not measured.

[a]Nonparenthetical values are experimental data; values in parentheses are calculated at 298 K, using B3LYP/6-31+G*. All values are enthalpies.

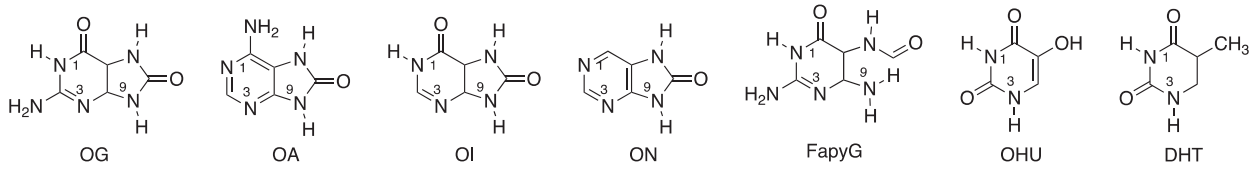

FIGURE 23 Fpg substrates. Fpg, formamidopyrimidine glycosylase.

TABLE 5 Calculated and experimental data for Fpg substrates (Kiruba et al., 2016)

	substrate	Calculated value[a]	Experimental value[b]
ΔH_{acid}[c]	5-Hydroxyuracil (OHU)	330.4	333
	Dihydrothymine (DHT)	347.1	349
PA[c]	5-Hydroxyuracil (OHU)	197.8	204
	Dihydrothymine (DHT)	200.7	205

[a]Calculated at 298 K, using B3LYP/6-31+G(d).

[b]Error is ±3–4 kcal/mol.

[c]All values are reported as enthalpies, in kcal/mol.

gas-phase experiments, not calculations, we will just briefly note that the computations establish that KIEs could be used to differentiate between a endocyclic and exocyclic mechanism for Fpg. The key is that the gas-phase experiments provided data that could be used to benchmark the calculations, so that the method and level could be trusted for the mechanistic KIE computations.

3.7 | Thymine DNA glycosylase

TDG excises thymine, as well as a "broad" range of bases from DNA mispairs (Figure 24). Its substrates include halogenated uracils, other pyrimidines, and even purines such as hypoxanthine. The acidity of the N1−H bond can reflect the ease of the *N*-glycosidic bond scission, just as with the other glycosylases: the more acidic the nucleobase, the better a leaving group its conjugate base should be (Bennett et al., 2006; Maiti et al., 2013). Krajewski and Lee worked on examining the thermochemical properties of 5-halouracils

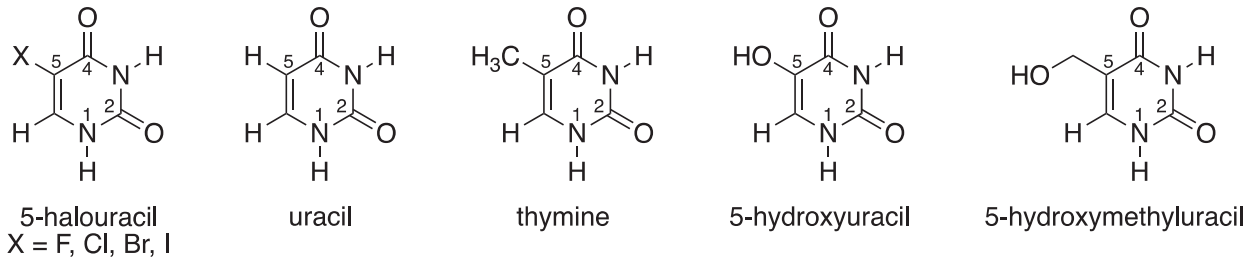

FIGURE 24 TDG substrates

TABLE 6 Calculated and experimental data for TDG substrates (Krajewski & Lee, 2021; Kurinovich & Phillips, Sharma, et al., 2002; Liu, Li, et al., 2008)

	Substrate	Calculated value[a]	Experimental value[b]
ΔH_{acid}[c]	5-Fluorouracil (5FU)	330.9	331 (331)
	5-Chlorouracil (5ClU)	328.6	330 (328)
	5-Bromouracil (5BrU)	327.6	326 (327)
	5-Iodouracil (5IU)	327.3	326 (326)
PA[c]	5-Fluorouracil (5FU)	201.9	202
	5-Chlorouracil (5ClU)	204.3	203
	5-Bromouracil (5BrU)	205.1	203
	5-Iodouracil (5IU)	206.6	205

Abbreviation: PA, proton affinity.

[a]Calculated at 298 K, using B3LYP/def2-TZVP.

[b]Experimental results are from bracketing; (Cooks results are available in parentheses). Error is ± 3−4 kcal/mol.

[c]All values are reported as enthalpies, in kcal/mol.

(Figure 24) computationally and experimentally (Table 6) (Krajewski & Lee, 2021). Comparison with experimental data confirmed that B3LYP/def2-TZVP is an accurate method to model the intrinsic properties of the halogenated substrates. After benchmarking these calculations with experimental data, the authors used calculations to establish the importance of stabilization of the O4 site by proton transfer or hydrogen bonding, in the enzyme mechanism.

4 | CONCLUSIONS

In this review, we have covered recent highlights of the use of gas-phase experiments, and more specifically, acidity and PA studies, to lend insight into catalytic mechanisms in organic and bio-organic chemistry. The gas-phase provides a unique environment that can both reveal intrinsic reactivity and mimic a hydrophobic environment in Nature. We are confident that future studies will continue to provide singular data that can be used to better understand catalysis.

REFERENCES

Bennett MT, Rodgers MT, Hebert AS, Ruslander LE, Eisele L, Drohat AC. Specificity of human thymine DNA glycosylase depends on N-glycosidic bond stability. *Journal of the American Chemical Society*. 2006;*128*(38):12510-12519.

Berti PJ, McCann JAB. Toward a detailed understanding of base excision repair enzymes: transition state and mechanistic analyses of N-glycoside hydrolysis and N-glycoside transfer. *Chemical Reviews*. 2006;*106*(2):506-555.

Bouchoux G, Sablier M, Berruyer-Penaud F. Obtaining thermochemical data by the extended kinetic method. *Journal of Mass Spectrometry*. 2004;*39*(9):986-997.

Breslow R. On the mechanism of thiamine action. IV.1 Evidence from studies on model systems. *Journal of the American Chemical Society*. 1958;*80*(14):3719-3726.

Brunel JM. BINOL: a versatile chiral reagent. *Chemical Reviews*. 2005;*105*(3):857-898.

Chandrasekhar V, Boomishankar R, Nagendran S. Recent developments in the synthesis and structure of organosilanols. *Chemical Reviews*. 2004;*104*(12):5847-5910.

Chen H, Justes DR, Cooks RG. Proton affinities of N-heterocyclic carbene super bases. *Organic Letters*. 2005;*7*(18):3949-3952.

Chen M, Moerdyk JP, Blake GA, Bielawski CW, Lee JK. Assessing the proton affinities of N,N'-diamidocarbenes. *The Journal of Organic Chemistry*. 2013;*78*(20):10452-10458.

Comita PB, Brauman JI. Gas-phase ion chemistry. *Science*. 1985;*227*(4689):863-869.

Cooks RG, Wong PSH. Kinetic method of making thermochemical determinations: advances and applications. *Accounts of Chemical Research*. 1998;*31*(7):379-386.

Damrauer R, Simon R, Krempp M. Effect of substituents on the gas-phase acidity of silanols. *Journal of the American Chemical Society*. 1991;*113*(12):4431-4435.

DePuy CH. Understanding organic gas-phase anion molecule reactions. *The Journal of Organic Chemistry*. 2002;*67*(8):2393-2401.

Dinner AR, Blackburn GM, Karplus M. Uracil-DNA glycosylase acts by substrate autocatalysis. *Nature*. 2001;*413*(6857):752-755.

Dondoni A, Massi A. Asymmetric organocatalysis: from infancy to adolescence. *Angewandte Chemie International Edition*. 2008;*47*(25):4638-4660.

Dong J, Drohat AC, Stivers JT, Pankiewicz KW, Carey PR. Raman spectroscopy of uracil DNA glycosylase−DNA complexes: insights into DNA damage recognition and catalysis. *Biochemistry*. 2000;*39*(43):13241-13250.

Drohat AC, Stivers JT. Escherichia coli uracil DNA glycosylase: NMR characterization of the short hydrogen bond from His187 to uracil O_2. *Biochemistry*. 2000a;*39*(39):11865−11875.

Drohat AC, Stivers JT. NMR evidence for an unusually low N1 pKa for uracil bound to uracil DNA glycosylase: implications for catalysis. *Journal of the American Chemical Society*. 2000b; *122*(8):1840−1841.

Enders D, Balensiefer T. Nucleophilic carbenes in asymmetric organocatalysis. *Accounts of Chemical Research*. 2004;*37*(8): 534-541.

Feng WY, Gronert S. 10 Gas-phase organic ion–molecule reaction chemistry. *Annual Reports Section "B" (Organic Chemistry)*. 2000;*96*:445-475.

Glasovac Z, Štrukil V, Eckert-Maksić M, Schröder D, Kaczorowska M, Schwarz H. Gas-phase proton affinities of guanidines with heteroalkyl side chains. *International Journal of Mass Spectrometry*. 2008;*270*(1):39-46.

Gronert S. Mass spectrometric studies of organic ion/molecule reactions. *Chemical Reviews*. 2001;*101*(2):329-360.

Hopkinson MN, Richter C, Schedler M, Glorius F. An overview of N-heterocyclic carbenes. *Nature*. 2014;*510*(7506):485-496.

Huang Y, Unni AK, Thadani AN, Rawal VH. Single enantiomers from a chiral-alcohol catalyst. *Nature*. 2003;*424*(6945):146.

Jiang YL, Drohat AC, Ichikawa Y, Stivers JT. Probing the limits of electrostatic catalysis by uracil DNA glycosylase using transition state mimicry and mutagenesis. *Journal of Biological Chemistry*. 2002;*277*(18):15385-15392.

Kaljurand I, Koppel IA, Kütt A, et al. Experimental gas-phase basicity scale of superbasic phosphazenes. *The Journal of Physical Chemistry A*. 2007;*111*(7):1245-1250.

Kee CW, Tan C-H. Chapter 23 chiral guanidines as asymmetric organocatalysts. In: North M, ed. *Sustainable catalysis: without metals or other endangered elements, Part 2*. The Royal Society of Chemistry; 2016:381-405.

Kimura E, Kitamura H, Koike T, Shiro M. Facile and selective electrostatic stabilization of uracil N(1)- anion by a proximate protonated amine: a chemical implication for why uracil N(1) is chosen for glycosylation site. *Journal of the American Chemical Society*. 1997;*119*(45):10909-10919.

Kiruba GS, Xu J, Zelikson V, Lee JK. Gas-phase studies of formamidopyrimidine glycosylase (Fpg) substrates. *Chemistry A Europe Journal*. 2016;*22*(11):3881-3890.

Kozmin SA, Rawal VH. Preparation and Diels−Alder reactivity of 1-amino-3-siloxy-1,3-butadienes. *The Journal of Organic Chemistry*. 1997;*62*(16):5252-5253.

Krajewski AE, Lee JK. Gas-phase experimental and computational studies of 5-halouracils: intrinsic properties and biological implications. *The Journal of Organic Chemistry*. 2021;*86*(9): 6361-6370.

Kurinovich MA, Lee JK. The acidity of uracil from the gas phase to solution: the coalescence of the N1 and N3 sites and implications for biological glycosylation. *Journal of the American Chemical Society*. 2000;*122*(26):6258-6262.

Kurinovich MA, Lee JK. The acidity of uracil and uracil analogs in the gas phase: four surprisingly acidic sites and biological implications. *Journal of the American Society for Mass Spectrometry*. 2002;*13*(8):985-995.

Kurinovich MA, Phillips LM, Sharma S, Lee JK. The gas-phase proton affinity of uracil: measuring multiple basic sites and implications for the enzyme mechanism of orotidine 5′-donophosphate decarboxylase. *Chemical Communications*. 2002;(20):2354-2355.

Lade JJ, Pardeshi SD, Vadagaonkar KS, Murugan K, Chaskar AC. The remarkable journey of catalysts from stoichiometric to catalytic quantity for allyltrimethylsilane inspired allylation of acetals, ketals, aldehydes and ketones. *RSC Advances*. 2017;*7*(13):8011-8033.

Leito I, Koppel IA, Koppel I, Kaupmees K, Tshepelevitsh S, Saame J. Basicity limits of neutral organic superbases. *Angewandte Chemie International Edition*. 2015;*54*(32):9262-9265.

List B. Introduction: organocatalysis. *Chemical Reviews*. 2007;*107*(12):5413-5415.

Liu M, Chen M, Zhang S, Yang I, Buckley B, Lee JK. Reactivity of carbene•phosphine dimers: proton affinity revisited. *Journal of Physical Organic Chemistry*. 2011a;*24*(10):929-936.

Liu M, Li T, Amegayibor FS, Cardoso DS, Fu Y, Lee JK. Gas-phase thermochemical properties of pyrimidine nucleobases. *The Journal of Organic Chemistry*. 2008b;*73*(23): 9283-9291.

Liu M, Tran NT, Franz AK, Lee JK. Gas-phase acidity studies of dual hydrogen-bonding organic silanols and organocatalysts. *The Journal of Organic Chemistry*. 2011b;*76*(17):7186-7194.

Liu M, Xu M, Lee JK. The acidity and proton affinity of the damaged base 1,N6-ethenoadenine in the gas phase versus in solution: intrinsic reactivity and biological implications. *The Journal of Organic Chemistry*. 2008a;*73*(15):5907-5914.

MacMillan DWC. The advent and development of organocatalysis. *Nature*. 2008;*455*(7211):304-308.

Maiti A, Michelson AZ, Armwood CJ, Lee JK, Drohat AC. Divergent mechanisms for enzymatic excision of 5-formylcytosine and 5-carboxylcytosine from DNA. *Journal of the American Chemical Society*. 2013;*135*(42):15813-15822.

Malkov AV, Barłóg M, Jewkes Y, Mikušek J, Kočovský P. Enantioselective allylation of α,β-unsaturated Aldehydes with allyltrichlorosilane catalyzed by METHOX. *The Journal of Organic Chemistry*. 2011;*76*(11):4800-4804.

Malkov AV, Bell M, Castelluzzo F, Kočovský P. METHOX: a new pyridine N-oxide organocatalyst for the asymmetric allylation of aldehydes with allyltrichlorosilanes. *Organic Letters*. 2005;*7*(15):3219-3222.

Malkov AV, Bell M, Vassieu M, Bugatti V, Kočovský P. New pyridine-derived N-oxides as chiral organocatalysts in asymmetric allylation of aldehydes. *Journal of Molecular Catalysis A: Chemical*. 2003;*196*(1):179-186.

Malkov AV, Dufková L, Farrugia L, Kočovský P. Quinox, a quinoline-type N-oxide, as organocatalyst in the asymmetric allylation of aromatic aldehydes with allyltrichlorosilanes: the role of Arene–Arene interactions. *Angewandte Chemie International Edition*. 2003;*42*(31):3674-3677.

Malkov AV, Ramírez-López P, Biedermannová L, et al. On the mechanism of asymmetric allylation of aldehydes with allyltrichlorosilanes catalyzed by QUINOX, a chiral isoquinoline N-oxide. *Journal of the American Chemical Society*. 2008;*130*(15):5341-5348.

Malkov AV, Stončius S, Bell M, et al. Mechanistic dichotomy in the asymmetric allylation of aldehydes with allyltrichlorosilanes catalyzed by chiral pyridine N-oxides. *Chemistry—A European Journal*. 2013;*19*(28):9167-9185.

Michelson AZ, Rozenberg A, Tian Y, et al. Gas-phase studies of substrates for the DNA mismatch repair enzyme MutY. *Journal of the American Chemical Society*. 2012;*134*(48):19839-19850.

Michelson AZ, Chen M, Wang K, Lee JK. Gas-phase studies of purine 3-methyladenine DNA glycosylase II (AlkA) substrates. *Journal of the American Chemical Society*. 2012;*134*(23):9622-9633.

Min T, Fettinger JC, Franz AK. Enantiocontrol with a hydrogen-bond directing pyrrolidinylsilanol catalyst. *ACS Catalysis*. 2012;*2*(8):1661-1666.

Miura D, Fujimura Y, Wariishi H. In situ metabolomic mass spectrometry imaging: recent advances and difficulties. *Journal of Proteomics*. 2012;*75*(16):5052-5060.

Moerdyk JP, Bielawski CW. Diamidocarbenes as versatile and reversible [2 + 1] cycloaddition reagents. *Nature Chemistry*. 2012;*4*(4):275-280.

Moerdyk JP, Bielawski CW. Reductive generation of stable, five-membered N,N′-diamidocarbenes. *Chemical Communications*. 2014;*50*(35):4551-4553.

Moerdyk JP, Schilter D, Bielawski CW. N,N′-Diamidocarbenes: isolable divalent carbons with bona fide carbene reactivity. *Accounts of Chemical Research*. 2016;*49*(8):1458-1468.

Moore JL, Rovis T. Carbene catalysts. In: List B, ed. *Asymmetric organocatalysis*. Berlin, Heidelberg: Springer Berlin Heidelberg; 2009:118-144.

Nakanishi K, Suzuki N, Yamazaki F. Ultraviolet spectra of N-heterocyclic systems. I. The anions of uracils. *Bulletin of the Chemical Society of Japan*. 1961;*34*(1):53-57.

Niu Y, Wang N, Munoz A, et al. Experimental and computational gas phase acidities of conjugate acids of triazolylidene carbenes: rationalizing subtle electronic effects. *Journal of the American Chemical Society*. 2017;*139*(42):14917-14930.

Pérez-Pérez J, Hernández-Balderas U, Martínez-Otero D, Jancik V. Bifunctional silanol-based HBD catalysts for CO_2 fixation into cyclic carbonates. *New Journal of Chemistry*. 2019;*43*(47):18525-18533.

Polyakova SM, Kunetskiy RA, Schröder D. Proton affinities of 2-iminoimidazolines with bulky N-alkyl-substituents. *International Journal of Mass Spectrometry*. 2012;*314*:13-17.

Puleo TR, Sujansky SJ, Wright SE, Bandar JS. Organic superbases in recent synthetic methodology research. *Chemistry—A European Journal*. 2021;*27*(13):4216-4229.

Radzicka A, Wolfenden R. A proficient enzyme. *Science*. 1995;*267*(5194):90-93.

Ren J-L, Zhang A-H, Kong L, Wang X-J. Advances in mass spectrometry-based metabolomics for investigation of metabolites. *RSC Advances*. 2018;*8*(40):22335-22350.

Sedgwick B. Repairing DNA-methylation damage. *Nature Reviews Molecular Cell Biology*. 2004;*5*(2):148−157.

Selig P. Guanidine organocatalysis. *Synthesis*. 2013;*45*(06):703-718.

Sharma S, Lee JK. Acidity of adenine and adenine derivatives and biological implications. A computational and experimental gas-phase study. *The Journal of Organic Chemistry*. 2002;*67*(24):8360-8365.

Sharma S, Lee JK. Gas-phase acidity studies of multiple sites of adenine and adenine derivatives. *The Journal of Organic Chemistry*. 2004;*69*(21):7018-7025.

Simonson T, Brooks CL. Charge screening and the dielectric constant of proteins: insights from molecular dynamics. *Journal of the American Chemical Society*. 1996;*118*(35):8452-8458.

Stetter H, Kuhlmann H. Addition of aliphatic aldehydes to activated double bonds. *Angewandte Chemie International Edition in English*. 1974;*13*(8):539.

Stivers JT, Jiang YL. A mechanistic perspective on the chemistry of DNA repair glycosylases. *Chemical Reviews*. 2003;*103*(7):2729-2760.

Sun X, Lee JK. Acidity and proton affinity of hypoxanthine in the gas phase versus in solution: intrinsic reactivity and biological implications. *The Journal of Organic Chemistry*. 2007;*72*:6548-6555.

Sun X, Lee JK. Stability of DNA duplexes containing hypoxanthine (inosine): gas versus solution phase and biological implications. *The Journal of Organic Chemistry*. 2010;*75*(6):1848-1854.

Tran NT, Min T, Franz AK. Silanediol hydrogen bonding activation of carbonyl compounds. *Chemistry—A European Journal*. 2011;*17*(36):9897-9900.

Váňa J, Roithová J, Kotora M, Beran P, Rulíšek L, Kočovský P. Proton affinities of organocatalysts derived from pyridine N-oxide. *Croatica Chemica Acta*. 2014;*87*(4):349-356.

Werner RM, Stivers JT. Kinetic isotope effect studies of the reaction catalyzed by uracil DNA glycosylase: evidence for an oxocarbenium ion−uracil anion intermediate. *Biochemistry*. 2000;*39*(46):14054−14064.

Wrzeszcz Z, Siedlecka R. Heteroaromatic N-oxides in asymmetric catalysis: a review. *Molecules*. 2020;*25*(2):330.

Zhachkina A, Lee JK. Uracil and thymine reactivity in the gas phase: the SN2 reaction and implications for electron delocalization in leaving groups. *Journal of the American Chemical Society*. 2009;*131*(51):18376-18385.

Zhachkina A, Liu M, Sun X, Amegayibor FS, Lee JK. Gas-phase thermochemical properties of the damaged base O(6)-methylguanine versus adenine and guanine. *The Journal of Organic Chemistry*. 2009;*74*(19):7429-7440.

AUTHOR BIOGRAPHIES

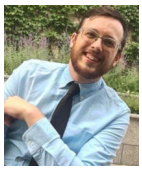

Damon J. Hinz received his BS from The University of Wisconsin-Milwaukee in 2017. In 2018, he joined the lab of Jeehiun Katherine Lee at Rutgers University, to pursue a Ph.D. He focuses on the studies of reactive intermediates and short-lived reactive species, using a combination of theoretical and gas phase mass spectrometric methods.

Lanxin Zhang received her BS at Wuhan University, China in 2016. She is pursuing a PhD in Chemistry under Dr. Jeehiun K. Lee at Rutgers, the State University of New Jersey. Her research focuses on the gas-phase studies of the reactivity of bioorganic substrates, using computational and mass spectrometric methods.

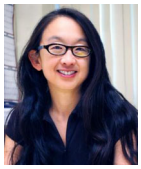

Jeehiun K. Lee received her BA at Cornell University (summa cum laude, Chemistry) and PhD at Harvard University (Organic Chemistry). After completing postdoctoral work with Professor Kendall Houk at the University of California, Los Angeles, she moved to Rutgers University, where she is now Professor of Chemistry. Her research is focused on combining gas-phase experimental and theoretical methods to interrogate the properties and reactivities of species of organochemical significance. Recent areas of interest are nucleophilicity, electrophilicity, and catalysis.

How to cite this article: Hinz DJ, Zhang L, Lee JK. Mass spectrometry in organic and bio-organic catalysis: using thermochemical properties to lend insight into mechanism. *Mass Spectrometry Reviews*, (2022);1-19.
https://doi.org/10.1002/mas.21797